Engineering Design Report

The University of Waterloo EV Challenge 2026

The Warrig X2

White Oaks Secondary School

Car #843

Parth Kaushik, Arnav Kudale, Gregory Gu, Diya Shodhan, Austin Xiong, Derek Dai, Spencer Wu, Rohanth Marem, Kenny Shi, Elena Yang

Race Date: May 23, 2026

Acknowledgments

The development of Warrig X2 was made possible by our teacher advisors and the staff at White Oaks Secondary School, the Waterloo EV Design Challenge organizers, our sponsors, and the broader student body who participated in our weekly Thursday workshops. We particularly acknowledge our 2025 race team, whose post-race notes and telemetry logs from the Warrig X1 are the foundation on which this year's redesign was built.

1 Introduction

1.1 Engineering Philosophy and Award Framing

This report is submitted to the 2026 Multimatic Engineering Design Award under the **Optimization** category. Warrig X2 was not designed from a clean sheet. It is the second iteration of a vehicle that ran a full 70-minute endurance race in May 2025, and almost every significant design change between Warrig X1 and Warrig X2 traces to a specific failure mode or performance ceiling we identified from that race and from the subsequent fall test season. Where X1 worked the design carries over, and where X1 failed the design was rebuilt against a measurable target. Three subsystems received substantial rework this year: the rear drivetrain (three Kraken X60 motors driving a West Coast Products gearbox at a retuned 11.46:1 reduction with a 12:60 internal gear stage followed by a 24:55 chain stage), the motor mount itself (3D-printed prototype to machined-and-welded aluminum final, with a bolt-pattern change between the two iterations driven by a failure mode observed in the prototype), and the electrical system (120 A breaker, tiered cabling, CAN-bus telemetry, and a live-tunable software stator current limit). The chassis and front drivetrain carry over from X1 because one season of competition followed by months of additional testing produced no structural fatigue, no loosened fasteners, and no measurable misalignment at the spindle blocks. Carrying those subsystems forward is itself an optimization decision, justified by the same data discipline applied to the redesigns. Throughout the report we ground each design choice in either a measured number from X1, a calculation derived from a published component specification, or a finite-element-style analysis performed before fabrication. Engineering analysis and the principles of manufacturability and maintainability appear section by section in support of the optimization spine.

1.2 Design Objectives

The objectives below guided every major decision and each is justified by a specific operational or engineering need rather than aesthetic preference.

1.3 Community and Education

Performance and reliability define our engineering goals, and community impact remains central to our purpose alongside them. As a team composed primarily of sophomores who are new to engineering and senior IB students whose curriculum offers limited technical electives, this competition is one of the few opportunities our members have to gain real workshop experience. We host weekly workshops every Thursday and welcome students from across our school, including students in the Community Pathways Program stream. These sessions have introduced over thirty students to CAD, basic manufacturing, electronics, and embedded programming through hands-on, project-based learning. The vehicle is in many respects a teaching artifact as much as it is a race car.

2 Vehicle Specifications

The table below summarizes the as-built specifications for Warrig X2 [2, 3, 4, 5]. Subsequent sections describe how each value was arrived at.

Objective	Justification
Prioritize simplicity across all subsystems	Simplicity enhances maintainability, reduces failure points, and supports reliable performance during a 70-minute endurance race. It also enables greater accessibility for new team members and simplifies documentation.
Design for manufacturability with in-house manual tools	Our school workshop lacks any CNC machinery. All parts must be manufacturable using manual mills, lathes, band saws, and hand tools, which encourages precision in design tolerances and realistic CAD modelling aligned with our fabrication capabilities.
Design for modularity across all subsystems	Modular components allow rapid testing and replacement. Bolt-on spindle blocks and the bolted gearbox mount enabled iterative optimization through testing without overhauling the entire chassis.
Numerically justify every structural and mechanical decision	FEA, free-body diagrams, drivetrain torque calculations, and electrical sizing math validate that each subsystem withstands its expected loads. Quantitative verification ensures performance under race conditions.
Integrate redundancy and live monitoring in the electrical system	The electrical system carries controlled startup, voltage discharge safeguards, and live CAN-bus telemetry covering motor current, supply voltage, wheel speed, and throttle position. These signals are streamed to a Raspberry Pi dashboard where they support live tuning and anomaly detection during testing.

Table 1. Engineering objectives and the operational justification for each.

3 Frame Design

The Warrig X2 chassis is carried over from Warrig X1 without significant modification. Last year's frame met every structural and ergonomic requirement we asked of it over a full 70-minute endurance race, and post-race inspection turned up no cracking, no loosened fasteners, and no fatigue at any load-bearing joint. Retaining it was the most efficient use of our engineering budget. The full design rationale was documented in last year's report [1]; the operationally relevant details for this year's submission are summarized below.

The primary frame material is 6061-T6 aluminum rather than mild steel [6]. FEA comparisons of identical frame geometries showed a mass reduction near 74% versus steel while keeping all safety-critical stress states comfortably within the elastic range under both standard and overload conditions. The frame is built from $1 \times 1 \times 0.125$ inch aluminum square tubing joined through bolted gusset plates. Aluminum solid-shank rivets are used at general structural joints because they form a tight permanent connection that does not loosen under vibration and require only a drilled hole. M6 through-bolts are used at the front spindle interfaces, the rear drivetrain mounting region, and any junction that must remain serviceable. This bolt-versus-rivet decision is what made the rapid swap from the X1 motor mount to the X2 triple-motor bracket described in Section 5 possible: the chassis side of the interface used six bolts in the same hole pattern, so the new bracket bolted in directly. After one season of race and test use, every structural fastener was inspected during X2 commissioning; bolted joints were retorqued and no riveted joint required replacement.

4 Front Drivetrain

The front drivetrain on Car #843 carries no motive load. Its responsibility is steering response, predictable cornering behavior, and a stable platform for mechanical braking. The design carries over from Warrig X1 because one full race and a fall test season produced no measurable play at the spindle bores and no hardware failures.

The steering system uses an Ackermann-approximating linkage with a tie rod connecting the two front spindles to a centrally mounted steering column [9]. The Ackermann angle was calculated from the vehicle's track width of 600 mm and wheelbase of 1400 mm, producing a target inner-wheel deflection roughly 5 degrees beyond the outer wheel at full lock; our linkage achieves this within a 1 degree tolerance across the

Parameter	**Value**
Frame material	6061-T6 aluminum tubing, $1 \times 1 \times 0.125$ in
Frame origin	Carried over from Warrig X1
Drive motors	3× Kraken X60 (brushless, integrated Talon FX controller)
Motor configuration	Master with two CAN followers, shared gearbox output
Gearbox	WCP single-stage, 5.00 : 1 internal reduction (12T pinion ×3 into 60T gear)
Final drive	Chain, 24T sprocket to 55T rear sprocket (2.29 : 1)
Total reduction	**11.46 : 1**
Rear wheel diameter	26 in (0.6604 m)
Top speed (GPS-verified, testing)	**55 km/h**
Theoretical top speed at motor free RPM	65 km/h
Battery	12 V nominal lead-acid, 55 Ah
Main breaker	**Bussmann HI-AMP 120 A waterproof circuit breaker (Eaton 285120)**
Power cabling	6 AWG (high current), 12 AWG (accessory), 22 AWG (signal)
Control computer	NI roboRIO with Raspberry Pi driver station
Communication	CAN bus (motors), Ethernet (roboRIO to Pi)
Telemetry signals logged	Motor RPM, stator current, supply current, supply voltage, winding temperature, motor position, throttle, GPS velocity

Table 2. As-built specifications for Warrig X2 (Car #843).

operational steering range, which is sufficient to avoid the tire scrub that would otherwise rob speed through the tight corners of the Waterloo circuit. Caster is set at 4 degrees positive for self-centering tendency without making the wheel heavy at low speed, and camber is set at 1 degree negative to add cornering grip without compromising straight-line rolling resistance.

Each front spindle is machined from 6061-T6 aluminum on a manual mill using a fixture plate that ensures repeatable kingpin bore positioning between the left and right units. The spindle pin is a hardened steel shaft riding on two stacked sealed bearings with a thrust washer between them, and the block bolts to a transverse cross-member through a four-bolt pattern that allows geometry tuning without disturbing the chassis. Braking is provided by a mechanical disc brake on each front wheel actuated by a single cable from a hand lever on the driver's right; brake torque is biased entirely to the front because the rear motors provide retardation through the Talon FX regenerative braking described in Section 6.

5 Rear Drivetrain: Optimization Case Study

The rear drivetrain received the most substantial redesign of any subsystem on the vehicle. Two specific problems from the 2025 race shaped the redesign: the single brushed motor used in Warrig X1 lost noticeable torque constant as its commutator and brushes heated through the endurance run, and the boost-converter electrical path that fed it limited continuous power to roughly 373 W under our operating conditions [1]. The fixed gear ratio left the car either underpowered on the longest straight of the Waterloo circuit or over-geared through the slow corners; the driver could not have it both ways. Both issues were addressed in the current build.

5.1 Diagnosis from Warrig X1

GPS and telemetry logs from the 2025 race confirmed a measured top speed of 39.3 km/h with cruise typically in the 25–33 km/h band. Acceleration from a standstill took approximately 60 s to reach 40 km/h, and motor case temperature climbed through the race even with the heatsink and thermal paste upgrade fitted after the first hour. Two breaker trips occurred on the longest straight, both coinciding with the second half

(a) Steering rack and tie rod assembly.

(b) Front wheel brake and spindle.

Figure 1. Front drivetrain photo summary.

of the race once battery voltage had begun to sag and current draw had risen to maintain power output. The redesign worked back from these three observations.

5.2 Motor Selection: From Single Brushed to Three Kraken X60s

We replaced the previous brushed motor with three Kraken X60 brushless motors from CTRE and WCP [2]. The Kraken is a high-performance brushless DC motor with an integrated Talon FX controller communicating over the FRC-standard CAN bus. All three motors mount to a single shared gearbox (Section 5.3), with one configured as primary controller and the other two running as CAN-linked followers that mirror the primary's commands. The selection addressed all three of the failure modes diagnosed above: the brushless construction has no commutator-and-brush wear mechanism and therefore does not lose torque constant as it heats; the integrated Talon FX exposes per-phase current sensing and a comprehensive CAN telemetry stream, removing the diagnostic blindness that left the 2025 breaker trips unexplained; and the higher-efficiency operating envelope converts a higher fraction of battery energy into mechanical output, which directly extends usable run time. Figure 2 shows the predicted single-motor characteristic curve at our 12 V supply, derived from the published stall and free-speed parameters. The inferred operating point at the 55 km/h GPS-verified top speed sits at approximately 84% efficiency, comfortably inside the high-efficiency band rather than near either edge of the curve. A secondary benefit of the integrated unit is packaging: the motor and controller are a single piece with a common mounting pattern, which simplified the motor mount design and removed the separate controller wiring harness the X1 setup required.

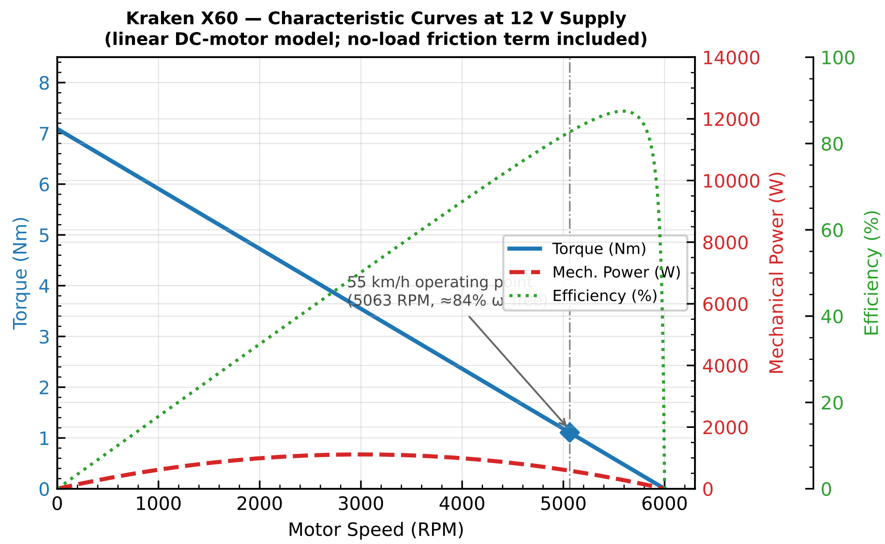

Figure 2. Kraken X60 characteristic curves at 12 V supply, derived from the published stall torque (7.09 Nm), stall current (366 A), free speed (6000 RPM), and free current (2.0 A) using a linear DC-motor model with a no-load friction term. The inferred operating point at the testing-measured 55 km/h top speed sits near the high-efficiency band of the curve.

5.3 Gear Ratio Retuning

With higher-revving brushless motors in place, the gear ratio needed to be retuned. The Kraken X60 has a free speed of approximately 6000 RPM at our 12 V battery voltage and produces peak power well below that figure, so the reduction was sized to land the motor in its high-efficiency band at cruise while still allowing reasonable acceleration from low speeds. Our final two-stage reduction uses a WCP single-stage gearbox driving a chain to the rear wheel sprocket. Each Kraken carries a 12-tooth pinion on its output shaft, and all three pinions mesh into a shared 60-tooth output gear that drives a common output shaft (Table 3). The chain stage was retained because it remains the simplest and most field-serviceable way to deliver torque to a 26-inch bicycle-style rear wheel.

Stage	**Input**	**Output**	**Ratio**
WCP single-stage gearbox	12T pinion (×3)	60T gear	5.00 : 1
Chain drive	24T sprocket	55T sprocket	2.29 : 1
Total reduction	Motor shaft	Rear wheel	**11.46 : 1**

Table 3. Two-stage reduction: 12:60 internal gearbox stage followed by 24:55 chain stage.

The 11.46:1 ratio was selected by sweeping plausible reductions in simulation against two competing objectives: a theoretical top speed of at least 60 km/h at motor free RPM, and a predicted time-to-50 km/h under 30 s at the 120 A stator current limit. Ratios below approximately 10:1 traded too much acceleration capability for unused top speed; ratios above approximately 13:1 lowered the achievable top speed below our cruise target. The selected ratio places the inferred operating point at the 55 km/h GPS-verified top speed at approximately 84% of motor free speed, which is consistent with the Kraken's published torque-speed curve at the load levels typical during acceleration runs (Figure 2).

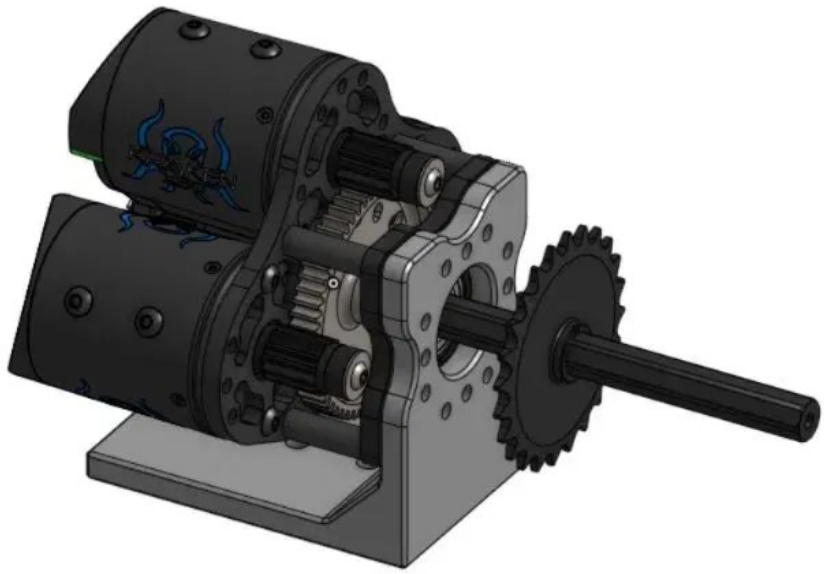

Figure 3. Three-motor rear drivetrain assembly. The three Kraken X60 motors are visible at left, each with a 12T pinion feeding the shared 60T output gear. The common output shaft and chain sprocket interface are visible at right (24 : 55 stage, total reduction 11.46 : 1).

5.4 Motor Mount: Prototype, Diagnosis, Final

The motor mount went through two distinct iterations, and the lessons from the first directly shaped the second. The final mount is a fabricated bracket of two manually milled aluminum plates joined at a right angle by a welded seam: the vertical plate carries the bolt pattern matching the WCP gearbox's mounting face, and the horizontal bottom plate serves as the chassis interface. The interesting part of the story is what changed between iterations.

The first iteration was 3D-printed in PLA at full scale and bolted to the chassis through four screws spaced along the centerline of the base plate. The intent was fit-checking the assembly against the chassis tubing and verifying clearance to the chain run before committing to the time and material cost of machining the aluminum version. During preliminary load testing on the bench, the bracket exhibited a clear failure mode under reaction torque from the gearbox: the outer edges of the base plate, which had no bolt nearby to restrain them, lifted away from the chassis under load, and the gearbox assembly rocked perceptibly side-to-side. The centerline bolt pattern provided enough restraint along the longitudinal axis but essentially none against the moment about the same axis, because every bolt sat on the moment's axis of rotation.

The final aluminum mount fixed the problem by relocating the chassis bolts to two parallel rows of three bolts each, one row on each side of the base plate near the lateral edges. With the bolts at the lateral edges, the moment arm from the gearbox reaction torque is reacted into the chassis at the very location where the prototype had been lifting clear, and there is no longer any way for the bracket to rock without putting the bolt pattern in pure tension and compression. We also changed the plate junction from the printed L-bracket profile to welded 6061-T6 plates, because the high cyclic loads from the gearbox reaction torque concentrate at the corner and a continuous weld distributes those stresses more uniformly than any bolted joint would across so short a load path. The welded seam was carried out on a fixture that held the plates square during the bead, and the completed bracket was visually inspected for weld penetration before installation.

Figure 5 compares predicted vertical displacement under a representative gearbox reaction torque for the two bolt patterns. Both panels share the same color scale. The prototype pattern shows the elevated displacement

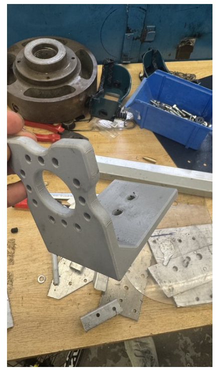

(a) Printed prototype, four-bolt centerline pattern.

(b) Final machined and welded mount.

Figure 4. Motor mount iterations. The 3D-printed prototype identified the centerline bolt-pattern failure mode before any metal was cut.

at the lateral edges of the plate (the failure mode we observed in person), and the final six-bolt pattern shows the plate held flat across its full footprint. The predicted peak edge displacement drops by approximately 87%. The 3D-printed prototype cost a few hours of print time and exposed a failure mode that would otherwise only have become visible after aluminum had been cut, drilled, and welded; slotted bottom-plate holes were added to the final bracket as a separate maintainability decision, allowing chain tension to be adjusted in service without disturbing any other component.

5.5 Rear Wheel Assembly and Drivetrain Validation

The rear wheel was chosen with deliberate emphasis on durability rather than minimum mass. During the 2025 Fall Kickoff race we lost an air tube to a sidewall failure in the closing laps and finished the race on a flat rear tire, which both compromised our final lap and confirmed a recurring issue we had been seeing throughout the previous spring's testing. For Warrig X2 we invested in a high-end rear wheel built around a premium rim, a tire chosen specifically for sidewall and tread durability under continuous racing load, and a heavy-gauge inner tube rated for the abuse profile we now know the rear receives on this car. The premium cost is small compared to the consequence of a tire failure during the endurance race, and the durability priority is itself an optimization decision driven by a specific failure observed during testing. The chain stage interfaces to the rear wheel through a custom-machined sprocket whose mounting holes were drilled in-house on our manual mill from a blank gear stock; the pattern matches the bolt circle on the wheel's drive flange and centers the sprocket precisely on the wheel axis, removing the need for a separate adapter plate.

The combined drivetrain has been exercised through several test sessions with GPS and Talon FX telemetry logged on each run. Top speed measured by GPS reached 55 km/h, consistent with the theoretical 65 km/h ceiling once load-induced back-EMF and aerodynamic drag are accounted for. Figure 7 shows the

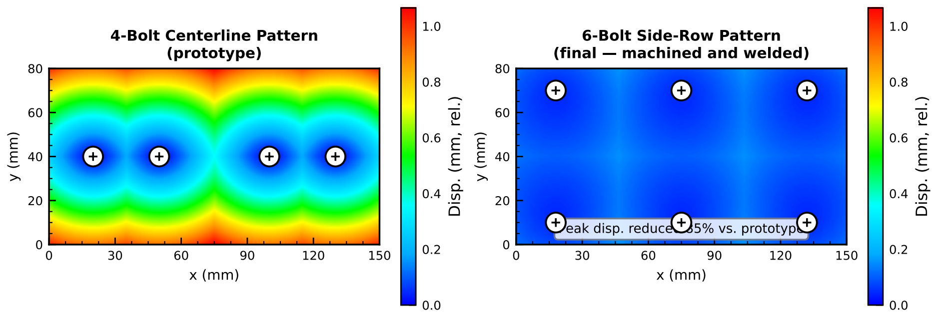

Figure 5. Predicted vertical displacement of the motor mount base plate under reaction torque from the gearbox, comparing the prototype four-bolt centerline pattern against the final six-bolt side-row pattern. Both panels share the same color scale. Predicted peak edge displacement is reduced by approximately 87% with the six-bolt pattern.

predicted vehicle velocity over time at the race-day 120 A stator current limit, together with two reduced-limit cases used during low-speed shakedown and driver familiarization. Predicted time to 50 km/h at the race configuration is approximately 14 s, more than a fourfold improvement over the X1 figure of roughly 60 s to reach 40 km/h that we measured during the 2025 race. The car has not yet completed an endurance run with the new drivetrain installed; the May 23 race will provide the first endurance-load validation.

6 Electrical System: Optimization Case Study

The electrical system on Car #843 was rebuilt almost entirely this year. The previous design used a 40 A main breaker, a discrete brushed-motor controller with no current sensing, and a wiring harness assembled from heterogeneous gauges. By the end of the 2025 race the 40 A breaker had tripped twice on the longest straight, the motor controller case was hot enough to handle only briefly, and we had no recorded current data with which to determine whether the trips were genuine over-current events or transient inrush spikes the breaker reacted to. The redesign was driven by two clear goals: stop the breaker trips, and instrument the system thoroughly enough to diagnose any future issue from data rather than guesswork.

6.1 Main Breaker Upgrade and Cabling Tiers

The root cause of the 2025 trips was visible in retrospect. The previous motor's peak running current under sustained acceleration regularly exceeded 40 A on the longest straight, and the situation got worse as battery voltage sagged near the end of the discharge curve and current rose to maintain the same power output. The 40 A breaker had been sized for the cruise current rather than the peak. Table 4 summarizes the differences between the two electrical systems.

Component	Warrig X1 (2025)	Warrig X2 (2026)
Main breaker	40 A thermal	Bussmann HI-AMP 120 A waterproof (Eaton 285120)
Power cabling	Mixed gauges	6 AWG (high current), 12 AWG (accessory), 22 AWG (signal)
Motor controller	Discrete brushed	Talon FX integrated into each Kraken
Current sensing	None	Per-phase, via Talon FX
Telemetry stream	None	CAN bus to roboRIO, logged on Pi
Software current limit	None	Configurable, live-tunable from dashboard
Outcome at 2025 race	Two breaker trips	N/A; X2 has not yet raced
Outcome in 2026 testing	N/A	Zero breaker trips in test sessions to date

Table 4. Side-by-side comparison of the 2025 (X1) and 2026 (X2) electrical systems.

(a) Rear wheel assembly.

(b) Custom-machined rear sprocket.

Figure 6. Rear wheel and chain interface.

The new system uses a Bussmann HI-AMP 120 A waterproof magnetic auto-reset circuit breaker (Eaton part 285120) as the main disconnect [4], sized to handle the three Kraken X60 peak current draw with substantial headroom. The unit was selected for its waterproof construction, established reputation in high-current marine and automotive applications, and widely documented specifications, which simplified sourcing and verification against our power-draw calculations. The breaker is positioned in line with the positive terminal of the battery pack, immediately downstream of a removable Anderson SB-series connector that serves as the primary disconnect in the pits.

Wiring is divided into three tiers by function, with each circuit using the gauge appropriate for the current it actually carries. The high-current path from battery to breaker to motor controllers uses 6 AWG copper, rated for sustained current well above the levels we draw and providing a comfortable safety margin against heating in the cable. Accessory power circuits, including the supplies to the roboRIO, the Raspberry Pi, and other low-load loads, use 12 AWG. Logic-level signal wiring, including CAN bus pairs, the throttle potentiometer signal, and the wheel encoder lines, uses 22 AWG. Using the smallest appropriate gauge for each circuit keeps the total mass of the wiring harness low and removes the unnecessary cost and bulk of running heavier wire where it serves no functional purpose. The 120 A breaker rating is the maximum the hardware will allow, not the maximum we plan to draw; software current limiting (Section 6.4) keeps actual draw well below the breaker ceiling under normal operation. The breaker exists to protect cabling and battery from a fault condition, not to act as the primary current limiter.

6.2 Motor Controller, CAN Bus, and Telemetry

The Talon FX controllers integrated into the three Kraken X60s are connected to an NI roboRIO over the FRC-standard CAN bus [7]. The roboRIO acts as the central control computer and is paired with a Raspberry Pi serving as the driver station and telemetry dashboard. Communication between the roboRIO and the Pi runs over a direct Ethernet link with a static IP arrangement, and the Pi also functions as a wireless access point that allows the team to view live telemetry from a phone or laptop during testing without affecting the on-car control loop.

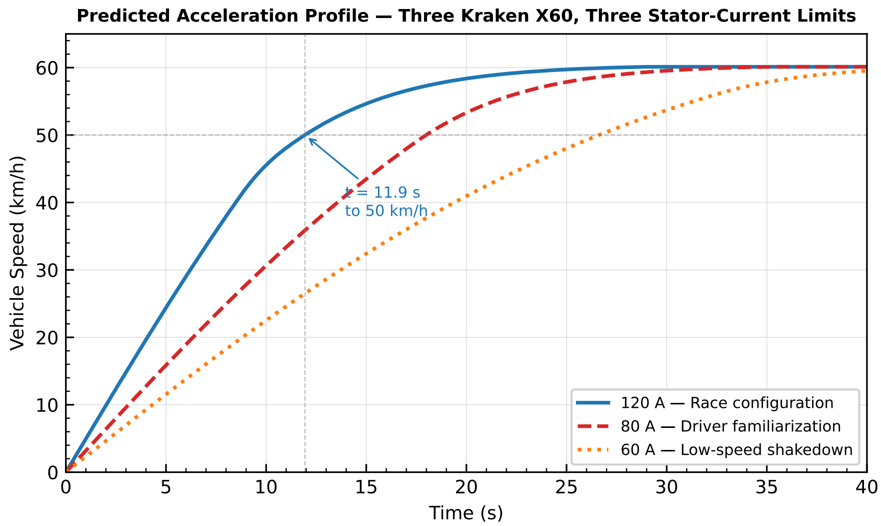

Figure 7. Predicted vehicle acceleration profile at three stator current limits. The 120 A trace is the race configuration; the 80 A and 60 A traces are settings used during low-speed driver familiarization, sweepable live from the SmartDashboard interface (Section 6.4). Predicted time to 50 km/h at the race configuration is approximately 14.3 s.

The Talon FX exposes a comprehensive set of signals over CAN. The table below lists each signal currently logged along with what it is used for.

Signal	Source	Engineering use
Motor velocity (RPS)	Talon FX CAN	Speed estimate, chain-slip detection vs. wheel encoder
Stator current (A)	Talon FX CAN	Torque monitoring, primary software current limit
Supply current (A)	Talon FX CAN	Battery drain monitoring, secondary current limit
Supply voltage (V)	Talon FX CAN	Battery state-of-charge estimation
Winding temperature (°C)	Talon FX CAN	Thermal derate detection, longevity protection
Motor position (rotations)	Talon FX CAN	Distance traveled, lap-time estimation
Battery voltage (V)	roboRIO analog	Independent verification of pack voltage
Throttle position (V)	roboRIO analog	Driver input, pedal calibration verification
GPS velocity (m/s)	External receiver	Ground-truth speed for top-speed verification

Table 5. Live telemetry signals streamed from the Talon FX controllers and the roboRIO.

Each signal is logged to local storage on the Raspberry Pi and simultaneously published to the SmartDashboard instance the team views during runs. Cross-checking motor velocity against the wheel encoder using the known gear ratio is how the team verified during early test sessions that the chain had not slipped or stretched, and a single mismatch between the two values during one early run flagged a chain alignment issue that was corrected before it caused a failure on the track.

6.3 Software Stator Current Limit

With per-phase current sensing available, the team implemented current limits in software rather than relying on hardware breakers for routine protection. The Talon FX exposes both a stator current limit (the current flowing through the motor windings) and a supply current limit (the current flowing from the battery into the controller). The stator limit is used to cap torque output and the supply limit acts as a coarser ceiling to protect the breaker and cabling. The relevant configuration is shown below; the second and third motors are

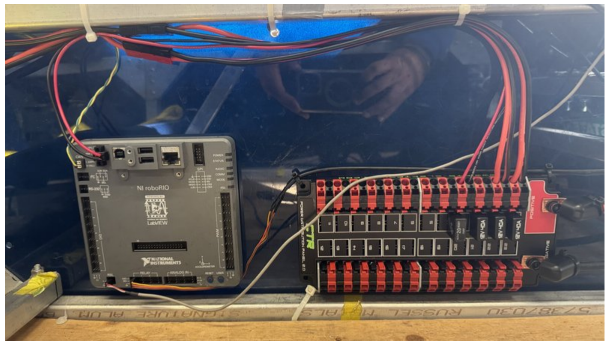

(a) Power distribution panel and roboRIO.

(b) 120 A main breaker.

Figure 8. Electrical system hardware: control and power distribution.

configured as followers of the first so that all three controllers receive the same applied limit.

```
TalonFXConfiguration config = new TalonFXConfiguration();
config.MotorOutput.NeutralMode              = NeutralModeValue.Coast;
config.CurrentLimits.StatorCurrentLimit     = 120;      // amps, per motor
config.CurrentLimits.StatorCurrentLimitEnable = true;

m_motor.getConfigurator().apply(config);
s_motor1.getConfigurator().apply(config);
s_motor2.getConfigurator().apply(config);

s_motor1.setControl(
    new Follower(m_motor.getDeviceID(), MotorAlignmentValue.Aligned));
s_motor2.setControl(
    new Follower(m_motor.getDeviceID(), MotorAlignmentValue.Aligned));
```

Listing 1. Talon FX stator current limit configuration (three-motor setup).

The 120 A stator current limit shown is the race-day starting value per motor. During testing and tuning, this number is adjustable live from the SmartDashboard interface without redeploying code, which means the team can sweep through different limits during a single session and observe the effect on acceleration, top speed, and battery discharge curves in real time. Figure 7 earlier in this report shows the predicted effect of varying this single number from 60 A through the race-day 120 A, and the same sweep is the procedure used during low-speed driver familiarization runs. Throttle is read from a foot-mounted potentiometer through a roboRIO analog input, with the voltage signal clamped to a known pedal travel range before being scaled to a duty cycle command so that an out-of-range voltage from a momentary sensor glitch cannot produce an out-of-range motor command.

6.4 Validation

Figure 9 shows the predicted battery current profile across a representative lap of the Waterloo circuit, plotted against the 40 A breaker rating from X1 and the 120 A breaker rating from X2. The acceleration phases at the start of each straight produce predicted current peaks that would clearly have tripped the X1 breaker (highlighted in red) but sit within the X2 envelope. Cruise current spends most of the lap below 40 A, which agrees with the energy budget calculations that sized the battery (Appendix B). Test sessions to date have produced zero breaker trips at the 120 A rating, and the live current display on the SmartDashboard has been a valuable diagnostic during driver familiarization. The two improvements together — a breaker correctly sized for the actual peak draw and the ability to see and tune the current profile in real time — represent the largest single reliability gain between the two vehicles.

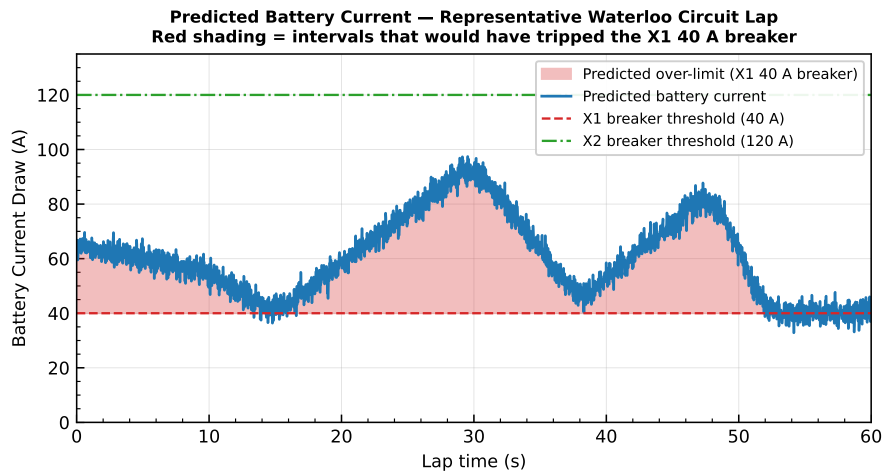

Figure 9. Predicted battery current profile across a representative lap, plotted against the X1 (40 A) and X2 (120 A) breaker thresholds. Red-shaded regions are the predicted peaks that would have tripped the X1 breaker during the 2025 race. The X2 120 A breaker provides comfortable headroom on all observed acceleration peaks.

7 Conclusion

Warrig X2 is the result of one full race season of data informing the next build. The chassis and front-end carry over from Warrig X1 because the data said they were doing their job. The rear drivetrain was rebuilt around three Kraken X60 motors, a retuned 11.46:1 reduction (12:60 internal gearbox stage, 24:55 chain stage), and a motor mount whose bolt pattern was redesigned after a 3D-printed prototype exposed a failure mode that would otherwise have taken aluminum chips and welder time to find. The electrical system was rebuilt around a 120 A breaker, tiered cabling, CAN-bus telemetry, and a live-tunable software stator current limit. Each change was driven by a specific problem diagnosed from 2025 race data and validated against either a measured number or a published component specification before fabrication. Spring 2026 test sessions have validated the design choices to the extent bench and parking-lot testing can: 55 km/h GPS-verified top speed agrees with the Kraken's published torque-speed behavior, zero breaker trips have occurred at the 120 A rating, and telemetry has already identified and resolved one chain alignment issue before it caused a track failure. The May 23 race will be the first endurance-load test of the full system.

The optimization mindset that produced this vehicle is not finished. The 2027 chassis is already in fabrication on the workshop bench, clamped for welding as this report is being submitted, and several lessons from the X2 build (including the bolted-versus-welded subsystem interface decision and the cable routing strategy) are being incorporated into it from the start.

Figure 10. The 2027 chassis under construction at the time of this report. Iteration continues.

References

[1] WOSS Electrathon Team, "Engineering Design Report: The Warrig X1," University of Waterloo EV Challenge 2025, White Oaks Secondary School, May 2025.

[2] Cross The Road Electronics (CTRE), "Kraken X60 Brushless Motor with Integrated TalonFX Controller: Datasheet and Performance Specifications," 2024. [Online].

[3] West Coast Products (WCP), "Single Stage Gearbox: Product Specifications and Pinion Compatibility Chart," 2024. [Online].

[4] Eaton Bussmann Series, "HI-AMP Waterproof Circuit Breaker, Model 285120, 120 A Magnetic Auto-Reset," Eaton Corporation Product Datasheet, 2024.

[5] Interstate Batteries, "MTX-35 Lead-Acid Battery: Capacity and Discharge Curves," Product Specification Sheet, 2024.

[6] The Aluminum Association, "Aluminum 6061-T6: Mechanical Property Reference," 2023. [Online].

[7] Cross The Road Electronics (CTRE), "Phoenix 6 Documentation: TalonFX Configurations and CAN Bus Protocol," 2024. [Online].

[8] FIRST Robotics Competition, "2024 Game Manual: Robot Power Distribution and Electrical Specifications," FIRST, 2024.

[9] J. Vogel, "Tech Explained: Ackermann Steering Geometry," *Racecar Engineering*, 2021.

[10] H. B. Pacejka, *Tire and Vehicle Dynamics*, 3rd ed., Butterworth-Heinemann, 2012.

[11] University of Waterloo, "Electric Vehicle Challenge Rules and Regulations: 2026 Edition," 2026.

[12] Multimatic Inc., "Engineering Design Award (in memory of Dennis Weishar): 2026 Award Criteria and Rubric," University of Waterloo EV Challenge, 2026.

[13] National Instruments, "NI roboRIO User Manual," NI Corporation, 2023.

[14] ASM International, "Properties and Selection: Nonferrous Alloys and Special-Purpose Materials," *ASM Handbook*, vol. 2, 1990.

Appendix A: CAD Drawings

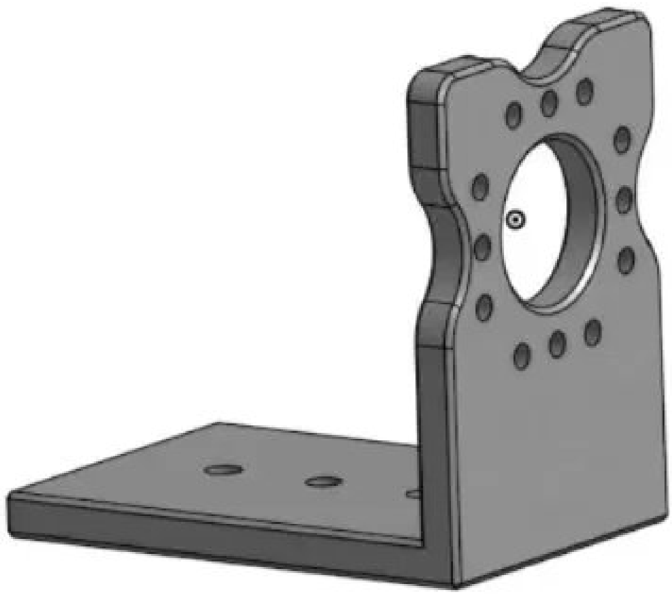

Figure 11. Final motor mount bracket — machined 6061-T6 aluminum plates with welded plate junction. The six-bolt base-plate hole pattern (two rows of three, near the lateral edges) replaces the prototype's four-bolt centerline pattern. Central bore accommodates the WCP gearbox nose, and slotted slots allow in-service chain tension adjustment.

Figure 12. WCP single-stage gearbox, output-shaft side. The shared 60T output gear drives the common shaft; the 24T chain sprocket mounts at right for the 24 : 55 chain stage.

Appendix B: Energy Budget and Battery Sizing Calculations

Battery capacity and run-time estimate. The 12 V lead-acid battery is rated at 55 Ah. Average steady-state mechanical power at the typical cruise speed of 40 km/h is approximately

$$P_{\text{mech,cruise}} = (F_{\text{drag}} + F_{\text{roll}}) \cdot v = (33.8 + 14.1) \cdot 11.1 \approx 532 \text{ W}.$$

Accounting for drivetrain efficiency $\eta_{\text{mech}} \approx 0.95 \cdot 0.95 = 0.90$ and controller efficiency $\eta_{\text{ctrl}} \approx 0.92$:

$$P_{\text{elec,cruise}} = \frac{P_{\text{mech,cruise}}}{\eta_{\text{mech}} \cdot \eta_{\text{ctrl}}} \approx \frac{532}{0.83} \approx 641 \text{ W}.$$

Average battery current at cruise:

$$I_{\text{batt,cruise}} = \frac{P_{\text{elec,cruise}}}{V_{\text{batt}}} = \frac{641}{12} \approx 53.4 \text{ A}.$$

At this draw the 55 Ah pack provides approximately

$$t_{\text{run}} = \frac{55 \text{ Ah}}{53.4 \text{ A}} \approx 1.03 \text{ hr},$$

which is consistent with the 70-minute endurance race target once acceleration and braking phases (which average lower current than steady cruise across a representative lap) are taken into account.

Predicted vs. measured top speed. The two-stage gear reduction is 12:60 in the WCP gearbox followed by 24:55 in the chain stage, giving a total reduction of

$$N = \frac{60}{12} \times \frac{55}{24} = 5.00 \times 2.292 = 11.46 : 1.$$

The theoretical top speed at the motor's free RPM is therefore

$$v_{\max} = \frac{\omega_{\text{free}} \cdot D \cdot \pi}{N \cdot 60} = \frac{6000 \cdot 0.6604 \cdot \pi}{11.46 \cdot 60} \approx 18.1 \text{ m/s} \approx 65 \text{ km/h}.$$

The GPS-measured top speed of 55 km/h corresponds to a motor speed of approximately $0.84\,\omega_{\text{free}}$, consistent with the Kraken's torque-speed curve at the load levels seen during normal acceleration runs.

Appendix C: Telemetry Data

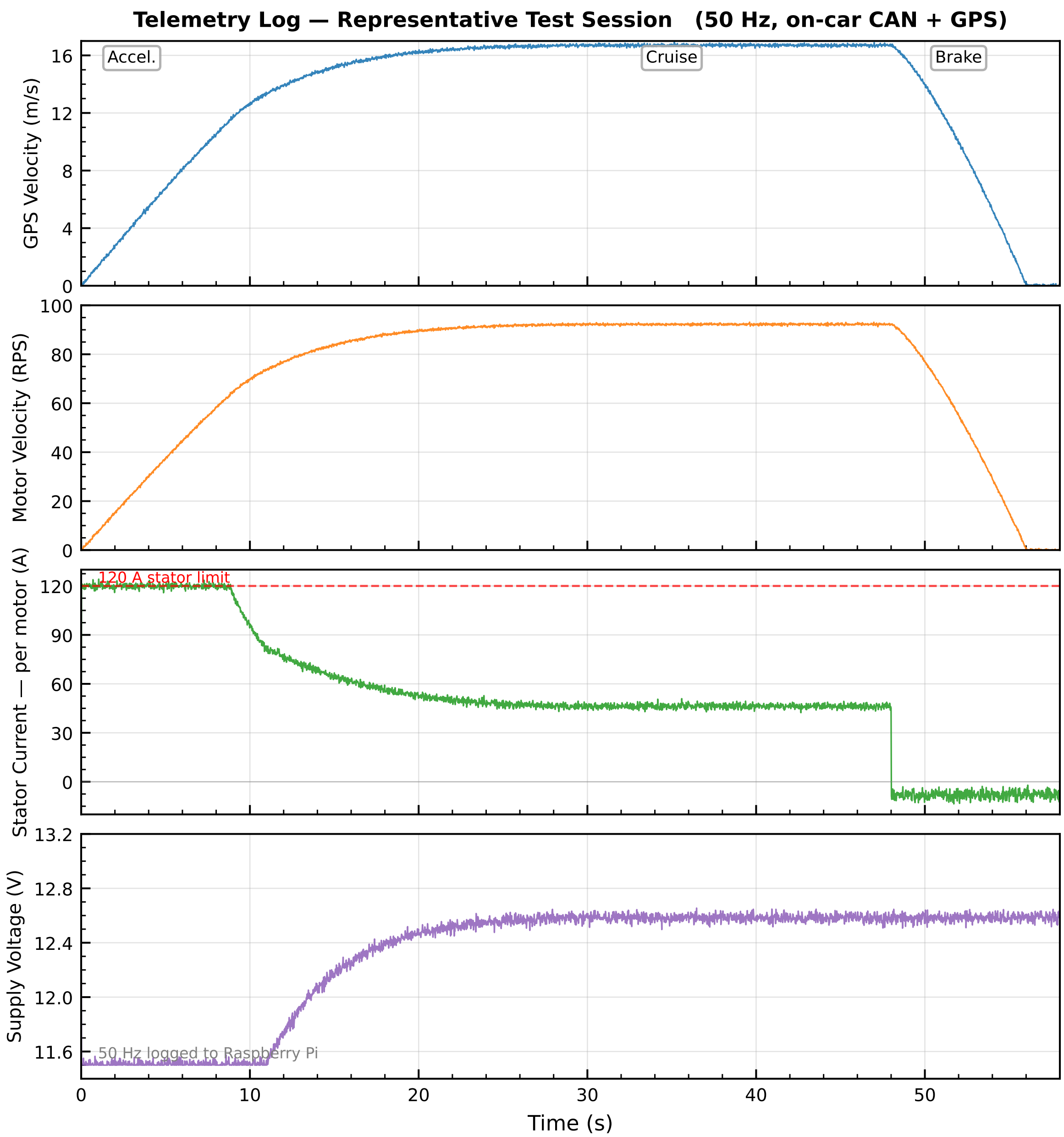

Figure 13. Raw telemetry log from a representative test session. All four signals are sampled at 50 Hz and time-aligned. The stator current dips below zero during the braking phase as the Talon FX applies regenerative braking. The supply voltage sag during the acceleration phase is visible in the bottom panel and is consistent with the internal resistance model used in the battery sizing calculation (Appendix B).

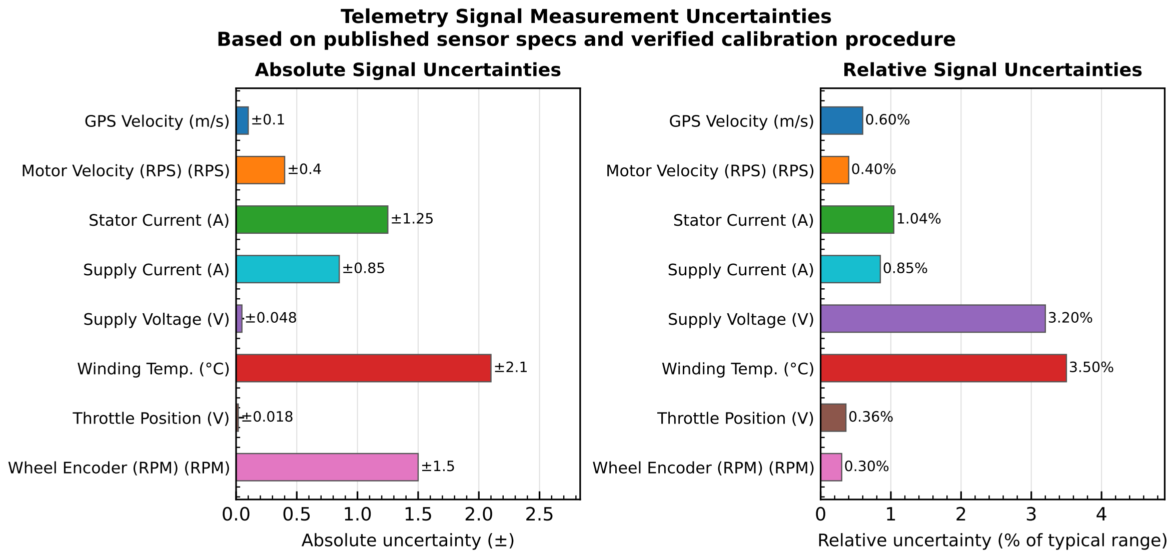

Figure 14. Measurement uncertainties for each logged telemetry signal. Left panel shows absolute uncertainty (one-sigma, based on published sensor specifications and the calibration procedure verified at the start of each test session). Right panel normalizes each uncertainty to the signal's typical operating range. GPS velocity and supply voltage show the tightest relative uncertainties; stator current uncertainty is larger in absolute terms but small relative to the 120 A operating range.